SPATIAL AND TEMPORAL CHARACTERISTICS OF SUPRA-GLACIAL MELT LAKES IN WEST-CENTRAL GREENLAND FROM SATELLITE OPTICAL REMOTE SENSING

THESIS

Presented in Partial Fulfillment of the Requirements for the Degree Masters of Science in the Graduate School of The Ohio State University

By

Nathanael Santos Amador, B.S.

****

The Ohio State University
2009

Thesis Committee:

Dr. Jason Box, Adviser

Dr. Ian Howat

Dr. Bryan Mark

Approved by

_____
Adviser

Atmospheric Sciences Graduate Program

ABSTRACT

Supra-glacial melt lakes form in the Greenland ice sheet ablation region in response to surface melt. The Jakobshavn Ablation Region (JAR) in west – central Greenland (68.2 – 68.8°N) is an area with a high areal concentration of melt lakes, providing an ideal region to study melt lake development. Moderate Resolution Imaging Spectroradiometer (MODIS) imagery are acquired for the 2000 – 2008 melt seasons (days 150 – 274) to observe the spatial and temporal melt lake characteristics. Knowing that melt rates vary with elevation, JAR is divided into five elevation zones of 250 m intervals, between 585 – 1835 m above sea level. An empirically-derived depth function, based on MODIS optical reflectance, is applied to classified melt lake pixels at JAR, yielding depth, area and volume statistics.

There is a strong correlation between melt lake area and volume quantities, regardless of elevation. Peak zonal fractional melt area, volume maxima and peak mean melt lake depth are reached at the mid-ablation zone (1035 – 1334 m). Melt intensity is determined from a Positive Degree Day (PDD) model. A correlation is found between melt lake area and volume anomalies and PDD anomalies that decrease with elevation.

The melt season at the uppermost elevation (1585 – 1834 m) begins five weeks after the onset at the lowest elevation (585 – 834 m). The date of maximum area and volume also increase with time, with a difference of 50 - 60 days. Average melt season at

JAR lasts 70 – 85 days below 1584 m and decreases to 30 days at the uppermost zone (1585 – 1834 m).

To verify MODIS-derived lake area accuracy, three IKONOS 1 m resolution images are compared for a single lake, Lake Disco (67.23°N, 48.61°W). Uncertainty in MODIS estimates of area are 20±2%. Such differences confirm the difficulty of identifying depth values between 0 and ~2.5 m from the Box and Ski (2007) lake depth-retrieval classification. Shallow depths prevent the MODIS sensor's coarse resolution from identifying lake perimeter in area estimation.

Sixteen melt lakes are identified on an elevation-basis to describe melt lake behavior at JAR lakes individually. Melt lakes reappear in the same basin year after year and lakes that form more frequently are found at lower elevations, while lakes at higher elevations form less frequently.

Overall, supra-glacial melt lakes in west-central Greenland show evidence of melt lake formation and evolution based on elevation and topography, as suggested by Lüthje et al. (2006) and McMillan et al. (2007). The highest rates of melt intensity occur at intermediate ablation zone elevations (835 – 1584 m), coinciding with larger area and volume quantities and a longer melt season duration. Anticipating continuing climate warming, it seems likely that the high ablation and lake formation in the mid-elevations (835 – 1584 m) will continue migrate towards the ice sheet interior.

To those who have been there, through thick and thin:

Mom and Apa

Grandma

AKNOWLEDGEMENTS

I first and foremost thank my adviser, Jason Box for his support and guidance along the way; teaching me what it is to be a glaciologist. Also, I thank Ian Howat and Bryan Mark for their time, effort and expertise. Thanks to David Porinchu, who has provided intellectual stimulation, comic relief and professional guidance. I thank Meng-Pai Hung, the IDL guru, who has provided me with continual support and solved my most crucial IDL problems.

I thank my parents, Santos and Lola Amador for their endless support (financially and emotionally) and motivation, even when I was feeling low. It is they who have made me who I am. Special thanks to my Grandma Lopez for being a third parent; for being there *whenever* I called and for random BuckID deposits.

I thank my network of friends for their comic relief, sanity checks and great 'family' dinners – Benjamin Gruber, Carl Kulpa, Sarah Pike, Elizabeth Reed and Estevan Santana. A special thanks to Paul Lockwood for being a great friend and mentor and also thanks to Scott Rowley, my best friend and partner. Thank you for your infinitesimal support and endless encouragement.

I finally thank my cohort for their intellectual support and numerous coffee breaks – Kyung-In Huh, Zoe Pearson and Kristin Walls and especially Karin Bumbaco. I thank Suzanna Klaf for our weekly brunches where she not only was a good friend but encouraged and guided me, both socially and academically.

VITA

7 July 1983……. Born – Fontana, California

2006…… B.S. Atmospheric Sciences, The Ohio State University

2006……..... Researcher – Remote Sensing Laboratory, The Ohio State University

2006 – *present*……. Graduate Research Associate, The Ohio State University

FIELDS OF STUDY

Major Field: Atmospheric Sciences

TABLE OF CONTENTS

Page

LIST OF TABLES

Table Page

LIST OF FIGURES

Figure Page

CHAPTER 1

INTRODUCTION

The Greenland ice sheet (Figure 1) is one of the largest freshwater reservoirs on the planet, containing an ice volume of ~2.5×10^6 km^3 or 10% of the world's total freshwater (Chen et al., 2006). Completely melting the ice sheet would raise global sea level by 7.4 m (Church et al., 2001; Chen et al., 2006), making the ice sheet mass balance an important component in the global hydrologic system and global freshwater budget. Greenland's area is approximately 1.6×10^6 km^2 with a maximum elevation located near the Summit Station, in central Greenland, situated at over 3 km above sea level (ASL) (Box, 2002). Despite its enormity, the Greenland ice sheet has been observed to be surprisingly sensitive to climate (Zwally et al., 2002; IPCC, 2007). A thorough understanding of ice sheet processes is vital to assessing Greenland's mass balance (Abdalati and Steffen, 2001).

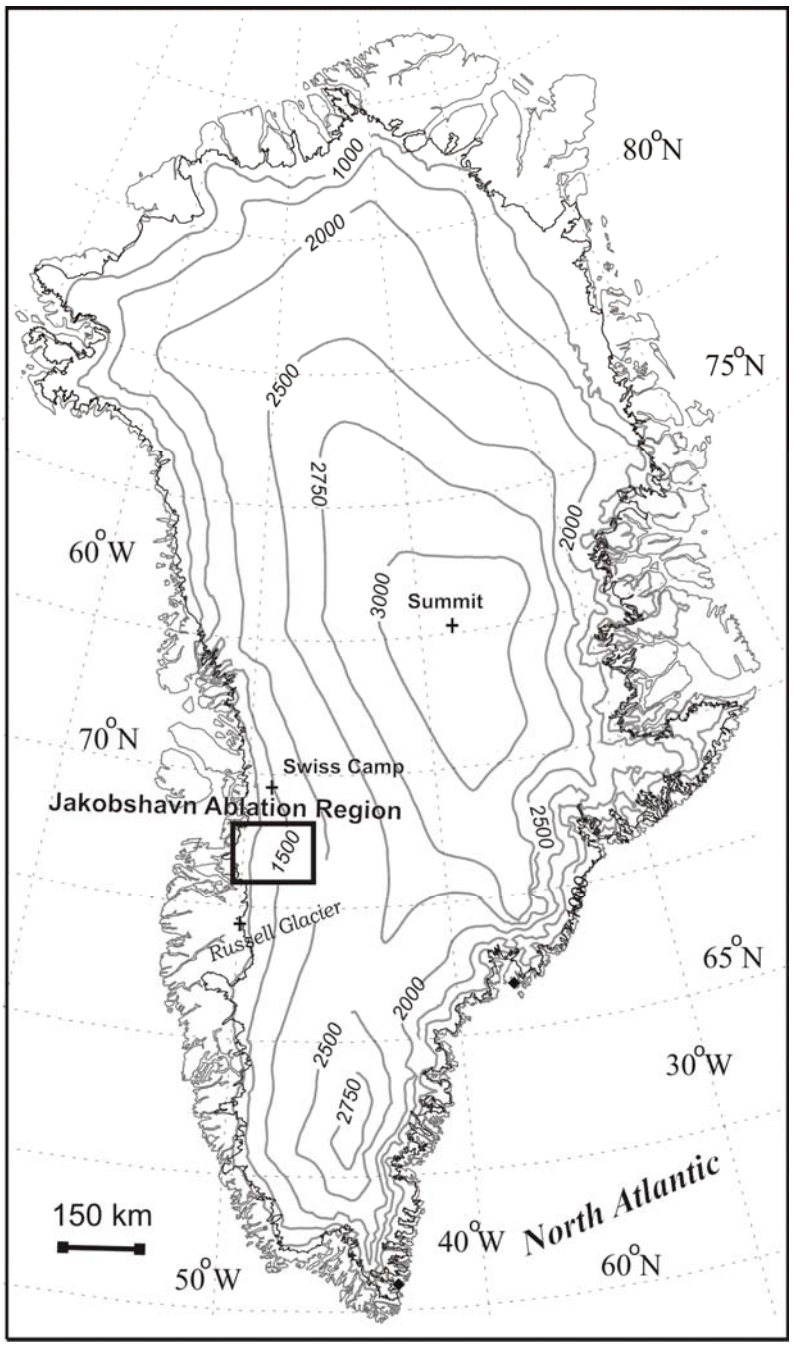

Figure 1. Greenland map featuring places referred to in this study. Inland ice sheet elevation contours (250 m) are included.

Variability in ice sheet mass balance affects the global climate system; specifically global sea level rise and freshwater input to the thermohaline circulation (Fichefet et al., 2003). Two principle components constituting Greenland's hydrological budget are the input of net snow accumulation and mass output from ablation (Paterson, 1994). Other components, such as surface blowing snow and water vapor fluxes, are 10 – 20% of the magnitude of precipitation (Box and Steffen, 2001) and discharge rates (Steffen and Box, 2001; Box et al., 2004).

Precipitation, in solid or liquid form, is the largest component of mass input on the ice sheet (Box et al., 2004). Accumulation rates vary more than an order of magnitude over the ice sheet, due to orography and continentality (Ohmura and Reeh, 1991; Ohmura et al. 1999), making it difficult to quantify precipitation rates in the ablation zone (Abdalati and Steffen, 2001; Box et al., 2004; Rignot et al., 2008). Melt water runoff accounts for roughly half of mass loss (Zwally and Giovinetto, 2001; Box et al., 2006), while the remainder is lost via calving at glacier termini, sub-glacial melting (Reeh et al., 1999; Rignot et al., 2008) , and surface and blowing snow water vapor fluxes (Box et al. 2004). Recent observations indicate an increase in the spatial and temporal melt extent (Abdalati and Steffen, 2001; Box et al., 2006; Hall et al., 2008), englacial runoff (Zwally et al, 2002) and ice discharge rates at marine-terminating glacier outlets (Joughin et al., 2008a; Rignot et al. 2008). A hydraulic lubrication mechanism is hypothesized to be the source of an observed acceleration in calving rates at outlet glaciers (Zwally et al., 2002, Alley et al., 2005; Rignot and Kanagaratnam, 2006; Rignot et al., 2008) while thermal forcing from the ocean (Holland et al. 2008) and glacier terminal stress balance changes

(Joughin et al. 2008b) are also important. Quantifying ice sheet response to climatic forcing is critical in the time-varying ice sheet mass budget of future climate warming scenarios.

1.1 THE JAKOBSHAVN ABLATION REGION

Jakobshavn Isbræ is a fast-moving, marine-terminating glacier, located in west-central Greenland (Echelmeyer and Harrison, 1990). Being one of the world's most productive glaciers in terms of iceberg discharge (Weidick and Bennicke, 2007). The Jakobshavn Isbrae lost a floating ice area of 10 km^2 in the 2008 melt season (http://bprc.osu.edu/MODIS/) following a larger breakup beginning in 2001 (Weidick et al., 2004). Glacial mass loss is observed via terminus retreat and marginal thinning (Abdalati and Steffen, 2001; Howat et al., 2007). The Jakobshavn Ablation Region (JAR) is situated in the central-western ablation zone of the ice sheet and is here defined as an area of 10,346 km^2, extending up to about 150 km inland and bounded by 68.2 – 68.8°N and 49 – 50°W, and an elevation range between 585 – 1835 m ASL (Figure 2).

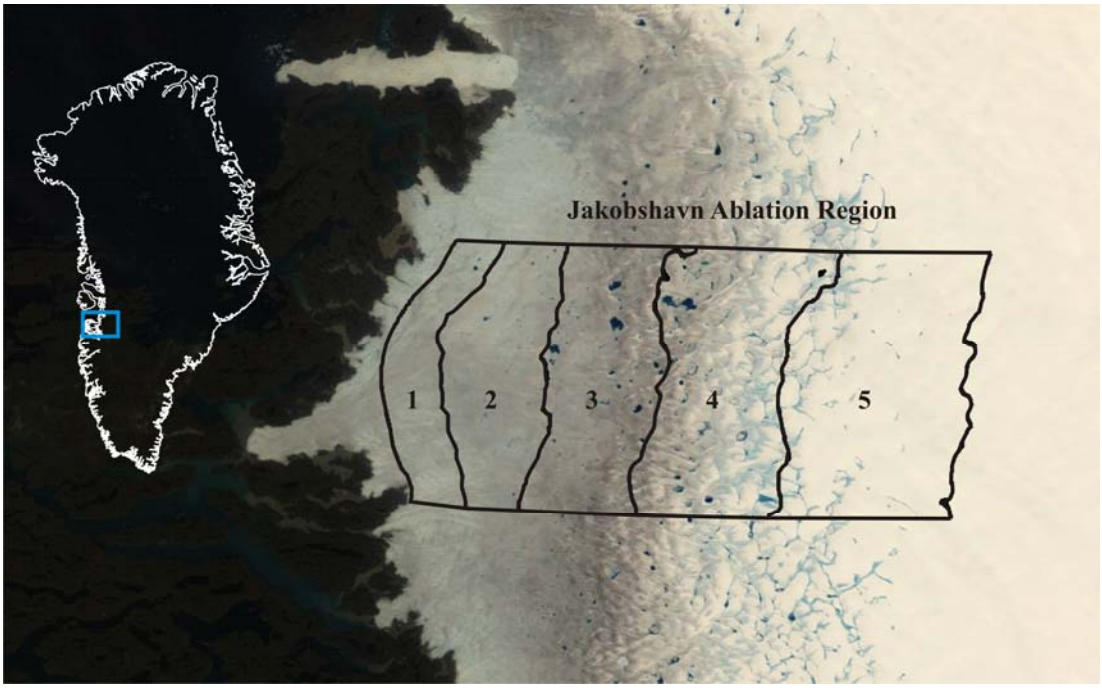

Figure 2. Jakobshavn Ablation Region (JAR) in west-central Greenland (68.2° - 68.8°N) partitioned into five elevation zones (250 m intervals) between 585 m and 1835 m ASL.

Year 2001 – 2006 mean summertime temperatures in JAR are estimated to be between -4° to 2°C (Hall et al., 2008). The frequency of above-freezing temperatures provides enough sensible heat in the near-surface atmosphere to promote sufficient surface melting to produce melt lakes. The melt season is bracketed between the onset and conclusion of melt. In this study, the melt season is identified as being between days 150 – 274, corresponding to 30 May – 1 October. During the melt season, supra-glacial melt lakes are found on the surface of the ice sheet in JAR.

1.2 SUPRA-GLACIAL MELT LAKES

Seasonal melting produces water that collects in undulation basins on the surface of the ice sheet (Lüthje et al., 2006; Box and Ski, 2007) forming supra-glacial melt lakes. Box and Ski (2007) have observed an area maximum of individual lakes of up to 10 km^2 at JAR. Lake area and volume are dependent on two principle factors; availability of melt water and ice sheet topography (Lüthje et al., 2006; McMillan et al. 2007). Looking at two catchment areas (22,000 km^2) near Swiss Camp (69°34′ N, 49°17′ W), and Russell Glacier (~67° N, ~48°W), McMillan et al. (2007) have estimated a total melt water production of these regions to be 2.696 km^3 during the 2001 melt season.

Ice sheet and outlet glacial flow speed has been linked with enhanced surface melt water supply via a lubrication mechanism (Zwally et al. 2002; Vieli et al., 2004; Das et al., 2008). Though melt water's role in ice sheet dynamics has been hypothesized (Joughin et al., 1996; Boon and Sharp, 2003; Parizek and Alley, 2005; Rignot and Kanagaratnam, 2006; Joughin et al., 2008), melt lake time-variation and dimensional characteristics, such as depth, area, and volume on the Greenland ice sheet, remain incompletely resolved. Studying JAR supra-glacial melt lakes provide a case study for a region characterized by a high concentration of melt lakes, a 1250 m elevation range and the close proximity to the active Jakobshavn glacier. Investigating supra-glacial melt lake behavior provides better understanding of the role surface melt water plays as a source of basal lubrication.

Many supra-glacial lakes, regardless of size, drain abruptly via outburst floods (Box et al., 1997; Bryzgis and Box, 2005; Box and Ski, 2007) suggesting an episodic and

non-linear role in their response to climate warming. The importance of melt lakes in ice dynamics seems clear, given that Joughin et al. (1996) found that rapid drainage of supra-glacial lakes was followed by accelerated glacier flow on the Ryder Glacier, in northern Greenland. Further, Das et al. (2008) found a sequence of lake drainage, glacial uplift and acceleration in ice discharge in the Jakobshavn ablation region.

While the sub-decadal record from daily, clear-sky MODIS imagery is too short in duration to determine long-term trends in melt lake area (Lüthje et al., 2006), a correlation of inter-annual anomalies in lake area and melt water production, if positive, implies an increased melt-lake throughput in likely future warming scenarios. The aim of this work is to make conclusive statements regarding the development of supra-glacial melt lakes when constrained spatially and temporally via the use of remote sensing. The question asked is *whether or not, and to what degree, melt lakes become important in a warming climate?*

CHAPTER 2

DATA

2.1 MODERATE RESOLUTION IMAGING SPECTRORADIOMETER IMAGERY

The primary dataset relied upon in this work comes from the Moderate Resolution Imaging Spectroradiometer (MODIS) sensor aboard NASA's Terra satellite (Solomonson et al., 1989) launched 18 December, 1999. At the writing of this thesis, MODIS has captured nine years (2000-2008) of quasi-daily imagery of Greenland. Imagery for a descending pass, times between 1345 – 1635 UTC (approximately 1045 – 1335 solar time over JAR), have been gathered as part of team work at the Byrd Polar Research Center. The Terra satellite passes over west-central Greenland during the melt season where solar elevation angle is between 29.4 – 48.9° (Box and Ski, 2007). Images acquired are clustered into two temporal segments, illustrating MODIS's 96.5 min orbiting period (Figure 3). MODIS orbits near-polar with an inclination of 98.2 degrees sun-synchronously at an altitude of 705 km above the equator (http://modis.gsfc.nasa.gov/).

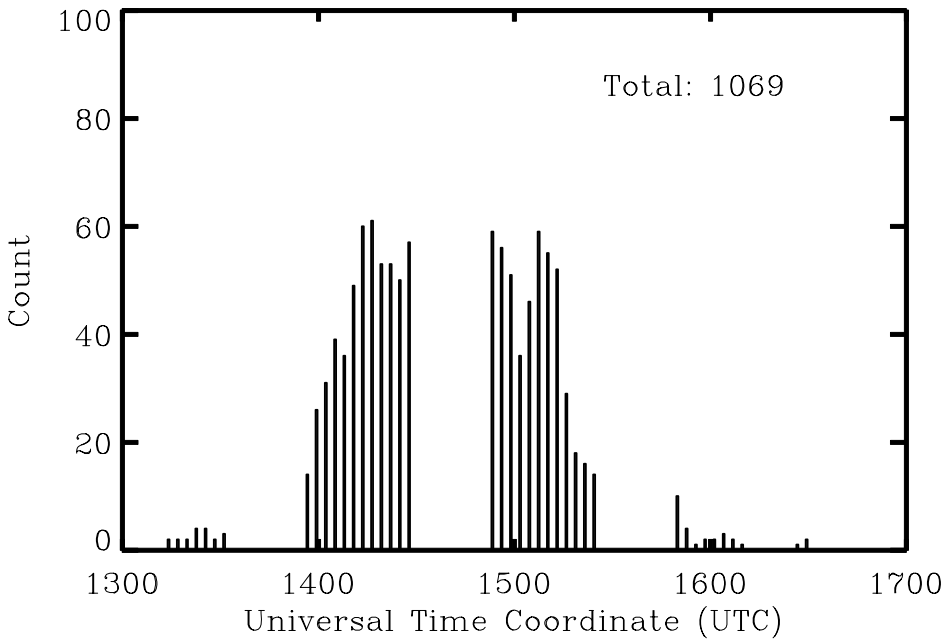

Figure 3. Universal time coordiantes (UTC) for year 2000 – 2008 melt season imagery used in this study.

Raw MODIS Level 1B calibrated radiances are available from NASA's Rapid Response System website: http://rapidfire.sci.gsfc.nasa.gov/realtime/. MODIS data used here include imagery in three optical bandwidths; band 1 (620–670 nm, red), band 3 (460–480 nm, blue), and band 4 (540– 570 nm, green). Here, bands 1, 3 and 4 are referred to as red (R), blue (B), and green (G), respectively. A procedure for MODIS optical imagery by Gumley (2003) is applied to re-sample blue and green bands originating at a 500 m resolution to the red band's 250 m resolution. Individual images do not contain information of previous surface conditions. Because melt lakes develop over time, repeat image acquisition is necessary. Figure 4 illustrates reprocessed 250 m optical imagery acquired over western Greenland from the MODIS sensor.

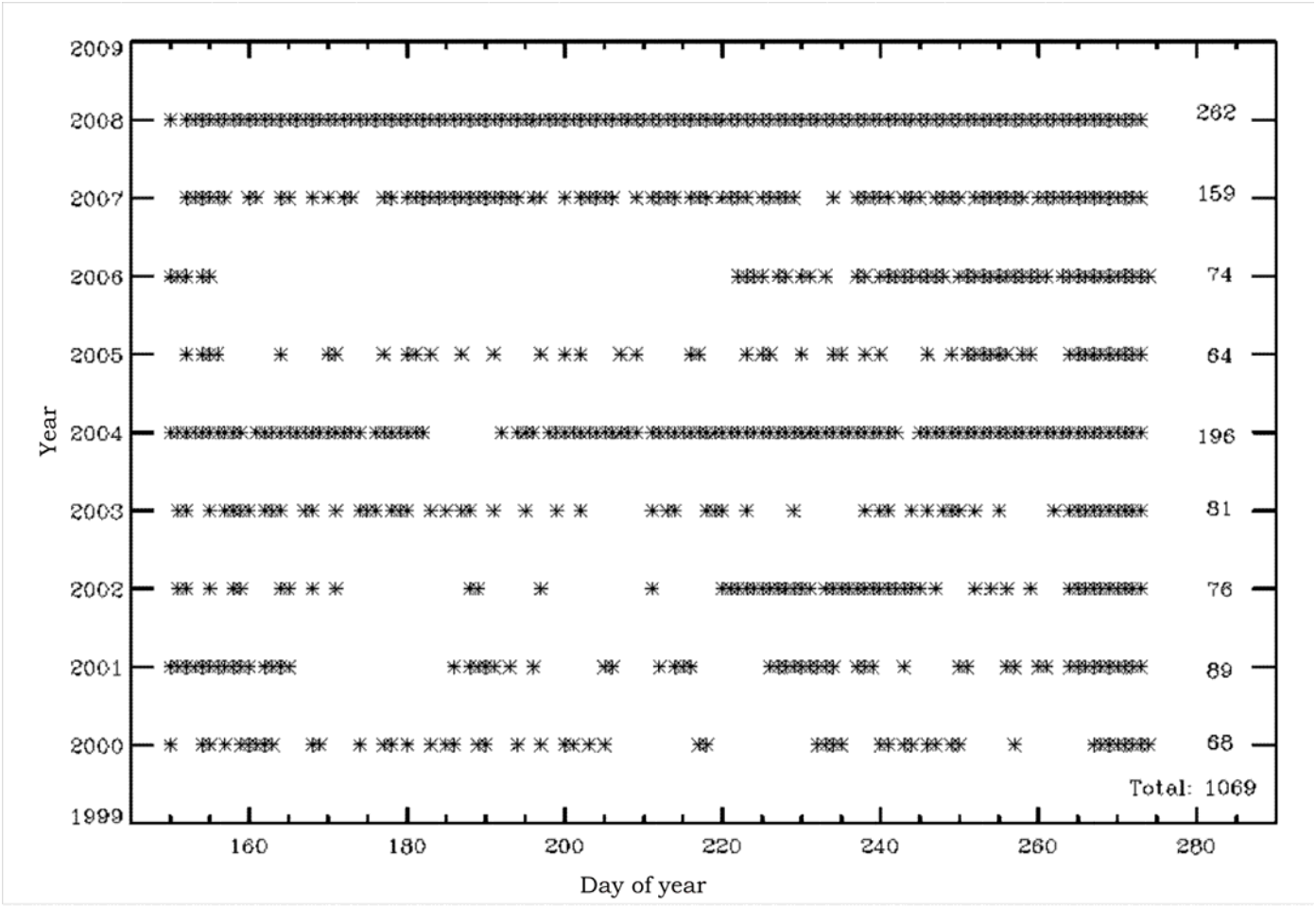

Figure 4. Reprocessed MODIS imagery for 2000 – 2008 melt seasons where each asterisk (*) represents an image acquisition date.

MODIS is an attractive data source for analysis at daily, seasonal, and inter-annual time scales due to its 2300 km swath width, adequate to image supra-glacial melt lake development at quasi-daily temporal resolution. Other remote sensors, such as Advanced Spaceborne Thermal Emission and Reflection Radiometer (ASTER), Landsat Enhanced Thematic Mapper (ETM) and IKONOS image the surface at higher resolution, making them useful for melt lake investigation. However, ASTER, Landsat ETM and IKONOS sensors have a lower temporal resolution (3 – 16 days) and swath widths between 11 and 185 km.

2.2 ELEVATION DATA

The digital elevation model (DEM) is based on that from Ekholm (1996). Uncertainties in the Ekholm DEM are ~15 m. The elevation data were gridded by J. Box to the 250 m grid used in this study.

2.3 COORDINATE GRIDS

Latitude and longitude grids are produced using the MODIS swatch-to-grid toolkit (MS2GT) (T. Haran, NSIDC, Boulder, CO). The use of the MS2GT allows for conversion of MODIS data from the dative Hierarchical Data Format – Earth Observing System (HDF-EOS) to projected, gridded output.

2.4 POLAR MM5

Regional climate models running in data assimilation mode offer observationally-constrained data over Greenland (Box et al., 2004; 2006). In this work, the fifth-

generation Pennsylvania State University-National Center for Atmospheric Research Mesoscale Model modified for use in Polar Regions (Polar MM5) (Bromwich et al. 2001; Cassano et al. 2001) is utilized as a source of data to quantify surface melt intensity. Surface air temperature is used in this work to relate melt lake development with surface climate. The model generates near-surface (2 m) daily mean air temperature and daily total positive degree grids at a 24 km resolution. Polar MM5 data was resampled by J. Box, using an MS2GT bi-linear interpolation routine named regrid, to the 250 m grid equivalent with the grid MODIS data are on.

2.5 LAKE SURVEYS

Surveys of two melt lakes, Lake A (69.53°N, 49.12°W) and Lake B (69.49°N, 49.21°W), were sponsored by Greenpeace and made by J. Box near Jakobshavn Glacier on 14-15 August, 2005. Lake surveys are compared with MODIS data for 16 August, depth and position measurements.

2.6 IKONOS High-Resolution Imagery

Three IKONOS images are used in this study. The images were acquired on days 201, 218 and 247 in 2007, or 20 July, 6 August and 4 September, respectively. The IKONOS imagery have 1 m spatial resolution.

2.7 MODIS DATA GAPS

MODIS data are not available for days 219 – 231 in 2000 and days 166 – 182 in 2001 due to sensor malfunction which forced the instrument to go to low power mode

and prevented the acquisition of data (B. Ridgway, NASA, personal communication, October, 2008). Cloud obstruction at JAR between days 171 – 187 in 2002 prevented the acquisition and reprocessing of MODIS imagery in this study.

MODIS data for days 158 – 221 in the 2006 melt season could not be processed using the Gumely (2003) methodology, due to problems with the MODIS HDF files. Given that most melt lake activity occurs before day 221 each year, exclusion of the 2006 MODIS data is necessary.

Clouds can obscure the surface in optical remotely sensed data. 84% of the 1069-count MODIS data set is removed using a cloud mask due to cloud obstruction at JAR. Repeat coverage of cloud-free MODIS imagery provides an average 6 day repeat pass (Box and Ski, 2007).

CHAPTER 3

METHODS

Remote sensing is used as a technique for Greenland ice sheet supra-glacial melt lake area and timing analysis (Sneed and Hamilton, 2006; Lüthje et al., 2006; Box and Ski, 2007; McMillan et al., 2007). Of dimensional variables, work has progressed to quantify water depth via satellite optical imagery (Sneed and Hamilton, 2006; Box and Ski, 2007).

3.1 ELEVATION ZONATION

Melt lake development varies with latitude, topography and elevation (Lüthje et al., 2006; McMillan et al., 2007). In this study, lake analyses are made among five elevation zones, each with a 250 m elevation range (Table 1). Latitudinal variability is minimized by selecting a limited (66 km) north-south extent (Figure 2).

Zone	Lower Boundary (m)	Upper Boundary (m)
1	585	834
2	835	1084
3	1085	1334
4	1335	1584
5	1585	1834

Table 1. Elevation of lower and upper boundaries for Jakobshavn Ablation Region elevation Zones 1 – 5.

3.2 IMAGE CLASSIFICATION

The use of optical band data can increase the skill in surface classification in remotely sensed imagery by looking at reflectance differences between the optical bands (red, green and blue). Sneed and Hamilton (2007) use ASTER optical band data to estimate depth and Box and Ski (2007) use MODIS optical band thresholds in lake classification and band ratios in depth retrieval.

In Box and Ski (2007), MODIS pixels are classified as flooded when red reflectance threshold values (R_T) are between 0.4 – 0.6 and the blue-to-red band ratio (B/R_T) is between 1.05 – 1.25. The classification scheme by Box and Ski (2007) is based on a relationship between MODIS optical reflectance and in-situ observations. This study uses default thresholds of $R_T = 0.49$ and $B/R_T = 1.08$ (Table 2). Factors such as surface

reflectance variability associated with water-saturated surface after rainfall or the effect of ice impurities, a.k.a. cryoconite dust (Gerdel and Drouet, 1960; Box and Ski, 2007) lead to varying thresholds. In this study, a lower R_T is used in 45% such cases, while a higher B/R_T is used in 25% such cases. A default cloudy case, where $R_T = 0.36$ and $B/R_T = 1.17$, is used for pixels that are visually-interpreted as misclassified flooded surface areas.

Case	R_T	B/R_T
1 (Default)	0.49	1.08
2 (Default Cloudy)	0.36	1.17

Table 2. List of cases and their relative values of the red threshold (R_T) and the blue-to-red ratio threshold (B/R_T) applied to the images for 2000 – 2008.

Lake classification is more sensitive to R_T than to B/R_T. Table 3 illustrates the zonal occurrence in which R_T is modified. When the lake classification scheme is applied, the average number of images per year with lakes evident at JAR is 21. A total of 172 images are found useful in this study over the 2000 – 2008 period. The image count on a zone-by-zone basis is illustrated in Table 4.

R_T	Zone 1		Zone 2		Zone 3		Zone 4		Zone 5	
	N	%	N	%	N	%	N	%	N	%
0.47	-	-	-	-	-	-	2	2.2	2	5.0
0.43	1	0.9	2	1.6	1	0.8	1	1.1	-	-
0.39	1	0.9	1	0.8	1	0.8	2	2.2	1	2.5
0.36	5	4.5	10	8.3	10	8.4	9	10.0	5	12.5
0.32	4	3.5	5	4.1	15	12.6	12	13.4	9	22.5
< 0.3	3	2.6	2	1.6	2	1.7	2	2.2	1	2.5

Table 3. The count (N) and percent of occurrence (%) where R_T is modified from default value $R_T = 0.49$ on a zone-by-zone basis.

Zone	1	2	3	4	5
Total Image Count	112	120	119	89	40
Average Annual Image Count	14	15	14	11	5
Average Repeat Coverage (days)	8	8	8	11	24

Table 4. The image count, average number of images per year and average repeat coverage for days with melt lakes present, divided into zones for years 2000 - 2008.

3.3 DEPTH – REFLECTANCE FUNCTION

Water depth at pixels classified as flooded is estimated using an empirical function available from Box and Ski (2007). Parameters for the Box and Ski (2007) depth-retrieval function are defined by data gathered at two lakes at JAR (Lake A and Lake B), located at ~69.5°N and in-situ data recorded on days 227-228 in 2005. Figure 5 illustrates the depth retrieval functions. Given that the Lake A and B functions are

similar, and in an effort to use a more general function, an average of the Lake A and B function is applied to melt lakes at JAR.

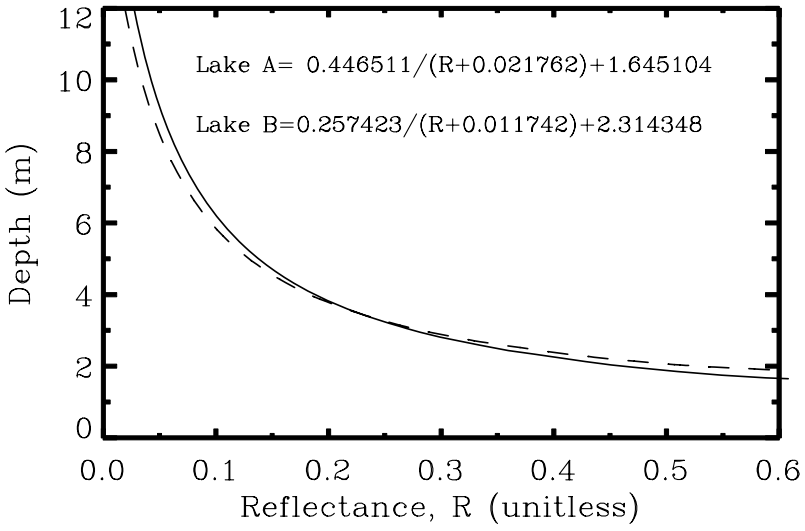

Figure 5. Lake A (solid) and Lake B (dotted) MODIS band 1 reflectance versus depth best-fit functions from Box and Ski (2007).

In-situ results from Box and Ski (2007) lake surveys provide depth sensitivity between ~2.5 – 11 m. Red reflectance is observed to be 0.6±0.1 as depth approaches 2.5 m. Uncertainty lies between depths of 0 and ~2.5 m which are lake perimeter. The slope of the function increases at lower reflectance values such that a small range in reflectance (< 0.1) can create large variability in depth estimation.

3.4 POSITIVE DEGREE DAY MODEL

Positive Degree Days (PDDs), useful in quantifying surface melt intensity (Braithwaite 1995; Braithwaite and Olesen, 1989; Zwally et al., 2002), are here quantified as the daily sum of hourly surface air temperature above the melting point. Polar MM5 model output is the source of near surface air temperature and therefore PDD values. Summation of Polar MM5 positive temperatures is made on eight 3-hourly intervals. Braithwaite and Olesen (1989) attribute PDD values as an 'ablation indicator' or melt intensity. It is recognized, however, that there can be a time lag between PDDs and the appearance of melt as the snow/ice surface temperature should first be raised to the melting point.

3.5 INTER-ANNUAL ANOMALY ANALYSIS

Lake area and volume statistics are evaluated in comparison to melt intensity. In order to avoid spurious correlation, average lake depth and total area and volume are computed per image and their deviation from the 8-year (2000-2008) mean is computed. Analysis of melt lake area and volume anomalies bypasses the hindrance of a short temporal period in determining trends.

3.6 CLASSIFICATOIN VALIDATION

MODIS-estimated melt lake area is verified with IKONOS 1 m spatial resolution imagery on a melt lake south of JAR, Lake Disco (67.23°N, 48.61°W). Nearly-coincident MODIS and IKONOS overpasses of Lake Disco facilitate checking the accuracy of the lake classification used in this study.

CHAPTER 4

MELT LAKE AREA VERIFICATION

The nearest cloud-free MODIS imagery of Lake Disco (67.23°N, 48.61°W) to the IKONOS days 201, 218 and 247 imagery is for days 204, 216 and 239, or with 23 July, 4 August and 27 August, 2007, respectively. Dates D1, D2, and D3 correspond to the three dates of nearest IKONOS and MODIS acquisition. In order to determine Lake Disco area from IKONOS imagery, a geospatial imaging tool, ENVI, is employed which allows for visually determining lake area.

The northwest sector (NWS) of Lake Disco is heavily concentrated with floating ice debris, clogging the drainage outlet (J. Box, personal communication, December, 2008). Inclusion of the NWS can affect total melt lake area estimates. On D1, estimate of total lake area (including NWS) is 3.37 km^2. Exclusion of the NWS provides an area of 2.21 km^2; a difference of 35%, or 1.16 km^2 (Figure 6).

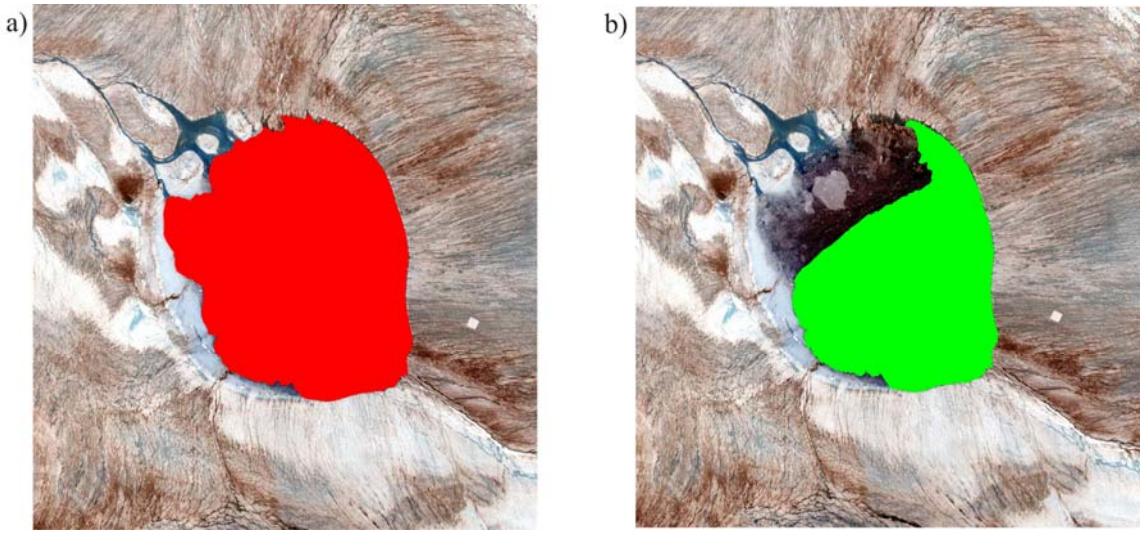

Figure 6. IKONOS 1 m resolution image of Lake Disco on day 201 (2007). Lake area is estimated including the (ice-cluttered) northwest sector (a) and without (b). The white square to the right of Lake Disco is the camp for which the 2007 boat surveys were launched (J. Box, personal communication, February, 2009).

Applying the default case of the depth-retrieval methodology where $R_T = 0.49$ and $B/R_T = 1.08$, Results using MODIS data of Lake Disco melt lake area on D1 to be 2.68 km^2 (Figure 7). Comparing the MODIS results for D1 to either estimate of IKONOS for D1 results in a difference of 20±2% (Table 5).

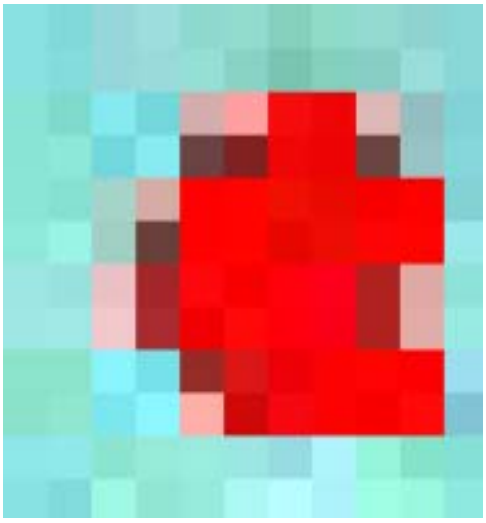

Figure 7. MODIS 250 m resolution image of Lake Disco on day 204 in 2007.

IKONOS area (km^2)	MODIS area (km^2)	Area Difference (%)
3.37 (northwest sector)	2.68	-20.5
2.21 (without)	2.68	21.2

Table 5. Estimates of Lake Disco by IKONOS (day 201) and by MODIS (day 204), along with the percent difference in area.

An area difference between IKONOS (Figure 8a) and MODIS (Figure 8b) on D2 is -18%. Lake Disco area estimated by IKONOS (Figure 8c) is underestimated by 22% by MODIS (Figure 8d) on D3.

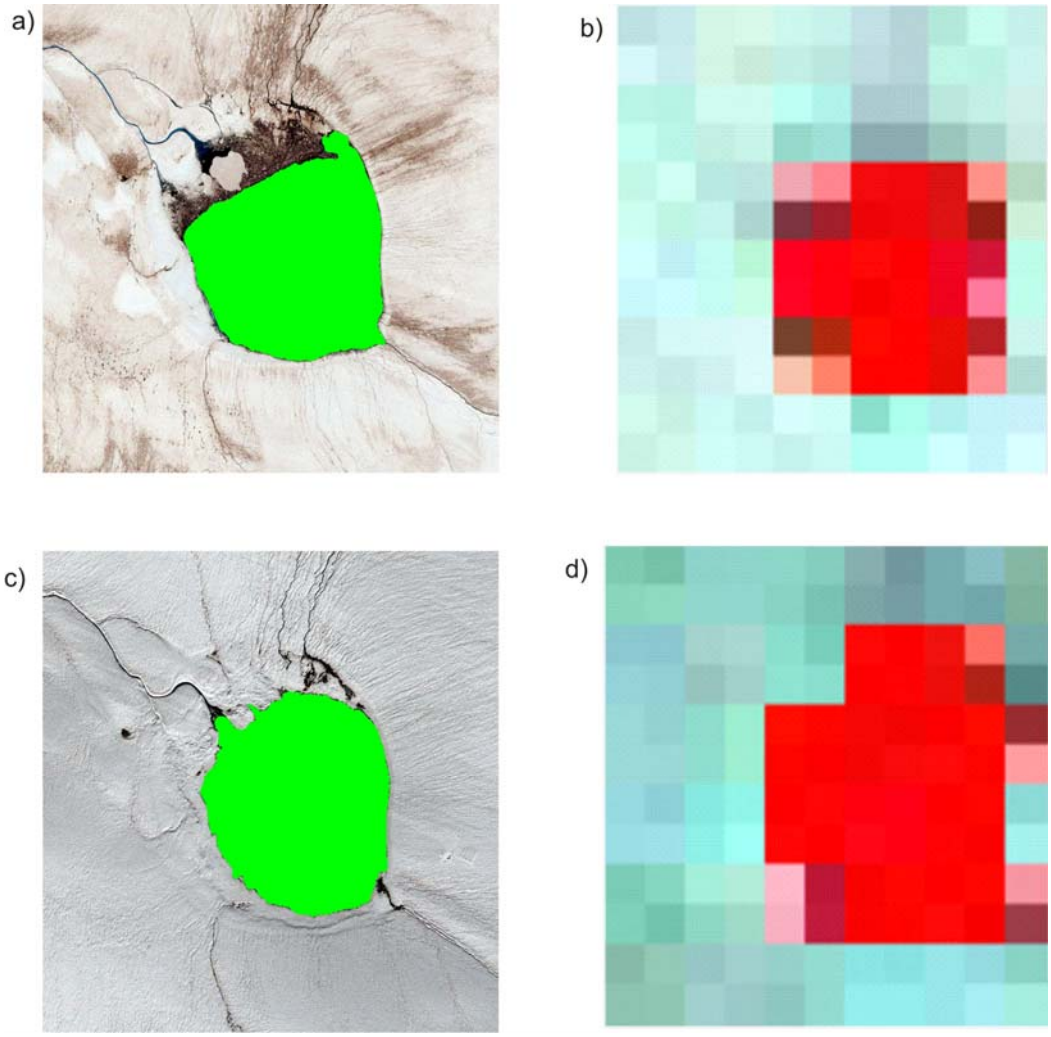

Figure 8. IKONOS and MODIS estimates of lake area for Lake Disco in 2007. IKONOS dates are on day a) 218 and c) 247. MODIS dates are on day b) 216 and d) 239. Scales are not equivalent between IKONOS images (a, c) and MODIS images (b, d).

For D1 – D3, MODIS estimates of Lake Disco are 20±2% from that of IKONOS-derived estimates. This is true too, for both cases (inclusion and exclusion) of the NWS. At this time of year (days 201 -247), precipitation is mostly in the form of snow and the

melt lake perimeters begin freezing (J. Box, personal communication). Variations in water properties change reflectance, thus causing MODIS to misclassify new lake boundaries. MODIS misclassification of lake perimeter is also caused by the depth-retrieval parameterization, where uncertainty lies when estimating depths of 0 to ~2.5 m.

When applying threshold values provided in (Table 3) the best-fit case to IKONOS estimates is where $R_T = 0.43$ and $B/R_T = 1.08$. Estimates for D1 and D3 have a negligible difference of ±0.03 km^2 (Figure 9). MODIS area estimates remain below that of IKONOS, regardless of changes in the R_T value. The ~20% underestimation of MODIS for Lake Disco on D2 may be attributable to differences in spatial resolution.

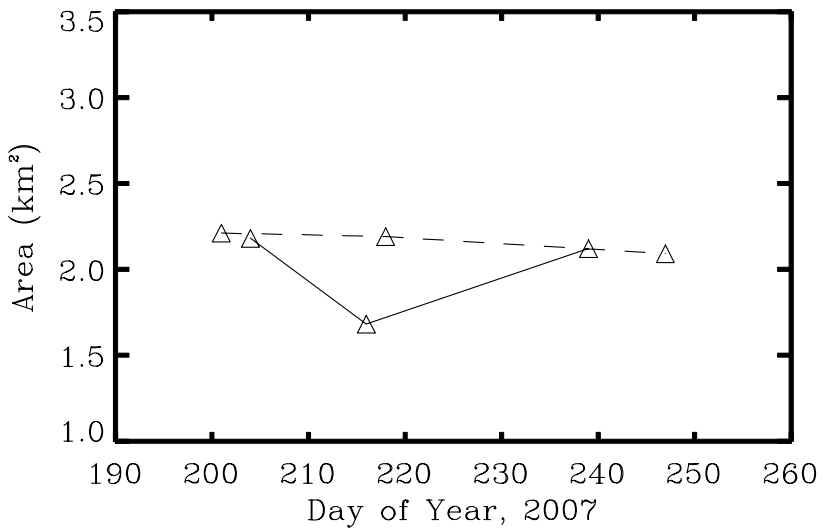

Figure 9. Area estimates by MODIS 250 m resolution (solid) and IKONOS 1 m resolution (dashed) (excluding the northwest sector) of Lake Disco during three days in the 2007 melt season. The case is where RT = 0.43 and B/RT = 1.08.

CHAPTER 5

MELT LAKE SPATIAL VARIABILITY

A high correlation (R = 0.96) is evident between melt lake area and volume from the Box and Ski (2007) parameterization (Figure 10). Similar results are evident at the other elevation zones (Table 6). This correlation is highest at Zone 2 (835 – 1084 m). The slope of the line represents the change in volume with the change in area, dV/dA (km^3km^{-2}). A close relationship between R and dV/dA values at JAR (585 – 1835 m) suggests quantities between lake area and volume are similar at all elevations within the ablation zone. The small range in dV/dA (0.015 km^3km^{-2}) suggests that no single lake type is favorable for any given elevation zone.

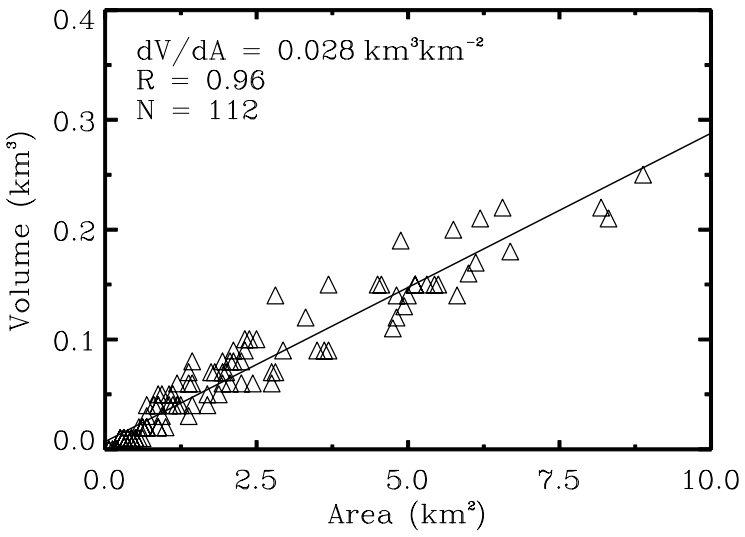

Figure 10. Correlation between melt lake area and melt lake volume for 2000 - 2008 images for the lowest elevation zone, Zone 1 (585 - 834 m).

Zone	1	2	3	4	5
Elevation (m)	585- 834	835-1084	1085-1334	1335- 1584	1585 - 1834
dV/dA (km^3km^{-2})	0.028	0.043	0.038	0.036	0.041
R	0.960	0.970	0.945	0.965	0.950

Table 6. Volume versus area (dV/dA) and correlation coefficient (R) for elevation zones 1 through 5.

Maximum fractional area coverage describes melt lake area behavior while removing the bias of elevation-based total area. Maximum fractional area coverage occurs in zones 3 and 4, that is, 4.2% and 3.6% of zonal area, respectively (Figure 11).

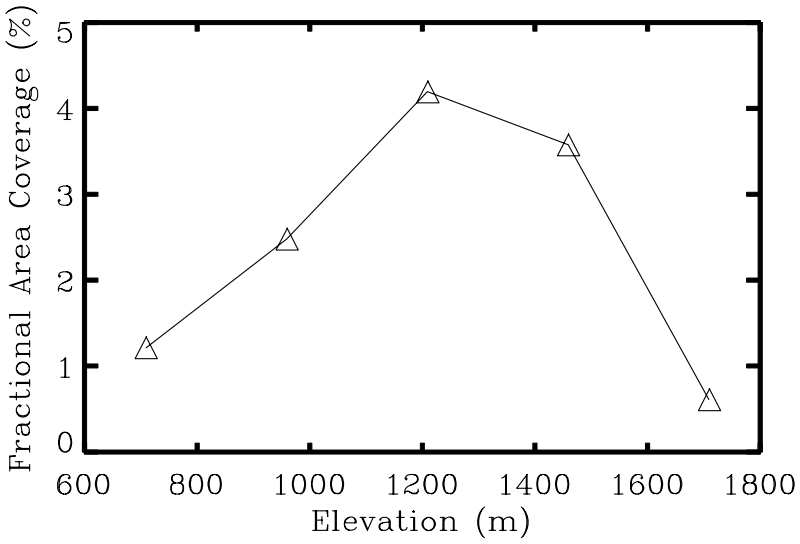

Figure 11. Maximum fractional melt lake area coverage (%) versus elevation for elevation zones 1 through 5 (585 – 1835m) between 2000 – 2008.

Maximum lake volume is observed in Zone 3 with a total value of 0.19 km^3 (Figure 12). Less water volume is evident in peripheral zones. A maximum volume of 0.45 km^2 at JAR (10,346 km^2) affirms estimates by Box and Ski (2007) where maximum volume in the western ablation zone (65.76 – 69.87°N) occurred on day 175, 2003 with a value of 1.284 km^3.

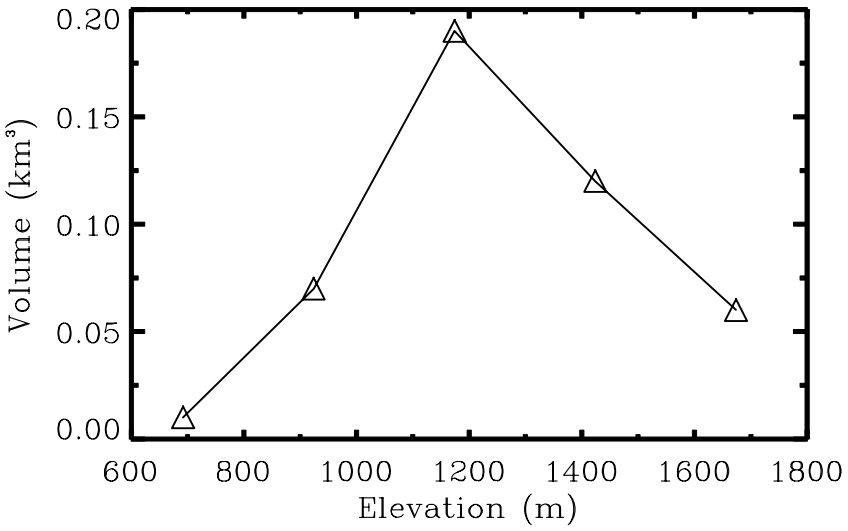

Figure 12. 2000 – 2008 maximum lake volume versus elevation for zones 1 through 5.

McMillan et al. (2007) estimate a cumulative summertime volume of 2.696 km^3 for 2001 for two glacier catchment areas totaling 22,000 km^2 near Swiss Camp (69°34′ N, 49°17′ W) and the Russell Glacier (~67° N, ~48°W). Results from this study, along with those from Box and Ski, 2007 and McMillan et al., 2007 signify that the ablation zone in west-central Greenland is highly active, producing several cubic kilometers of melt water which can enhance basal sliding.

A combination of melt lake area maxima, zonal fractional area and melt lake volume indicates that elevations between 1085 – 1584 m are most conducive to high melt lake volume. These results are consistent with the implication by McMillan et al. (2007) and Lüthje et al. (2006) that elevation and topography affect lake volume. If both area

and volume are maximized in Zones 3 and 4, it is expected that mean melt lake depth is greater at such elevations.

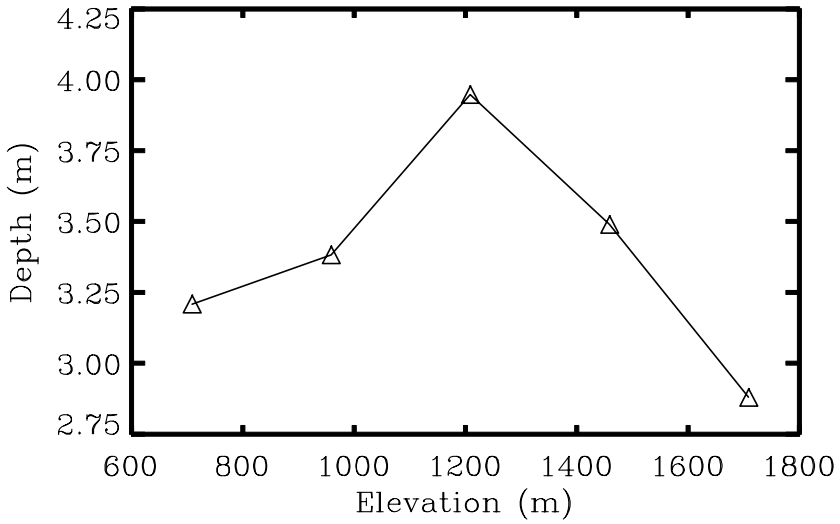

Figure 13. Mean lake depth versus elevation for elevation zones 1 – 5 (585 – 1834 m) for 2000 - 2008.

Average lake depth peaks at 1085 - 1335 m elevation (Figure 13), an altitude near the equilibrium line altitude (ELA) (Ohmura et al., 1995). A lower average depth in Zone 1 is attributable to a steeper slope. Since Zone 1 is the narrowest zone (Figure 2) with a width of ~25 km, it is believed that lake depths approaching 3.25 m are inhibited by topography and begin to spill over. A minimum average depth, occurring at the highest elevation zone (Zone 5) may be due to lower surface ablation rates above the ELA, due to lower mean surface temperature and higher surface albedo (van den Broeke et al., 2008). Above the ELA, the surface of the ice sheet is dominated by wet snow while below the

ELA, the surface is bare ice. A gradual slope above the ELA is conducive to less undulation formation at higher elevations. The combination of a wet snow surface type and less undulation above the ELA may be the cause for lesser lake area and shallower mean depth values in Zone 5 (1585 – 1834 m).

Maximum depth in this study is 10.37 m and is observed at Zone 3 on day 218, 2000, which may be an underestimate in 'true' lake depth as the Box and Ski (2007) depth parameterization loses sensitivity to optical reflectance near 11 m. Further, depths of up to 15.5 m have been observed in 2007 boat surveys (J. Box, personal communication, February, 2009).

A relationship is found between inter-annual anomalies of both surface melt intensity and melt lake area (Figure 14). Scatter in area amplifies with increasing melt intensity anomaly, suggesting that the temperature on the image date is not the only explanatory factor. Lake area or volume responds to past days and weeks of surface climate forcing. The dispersion of scatter suggests that most lakes are responsive to melt intensity. Instances of insensitive lakes occur when there is high melt intensity and low melt area. These instances are concentrated in the first half of the melt season. In Zone 1 and Zone 2, instances of low melt area sensitivity to high melt intensity occur between days 150 – 198 and 169 – 214, respectively. These instances exemplify the fact that melt lake area responds to meteorological forcing over time.

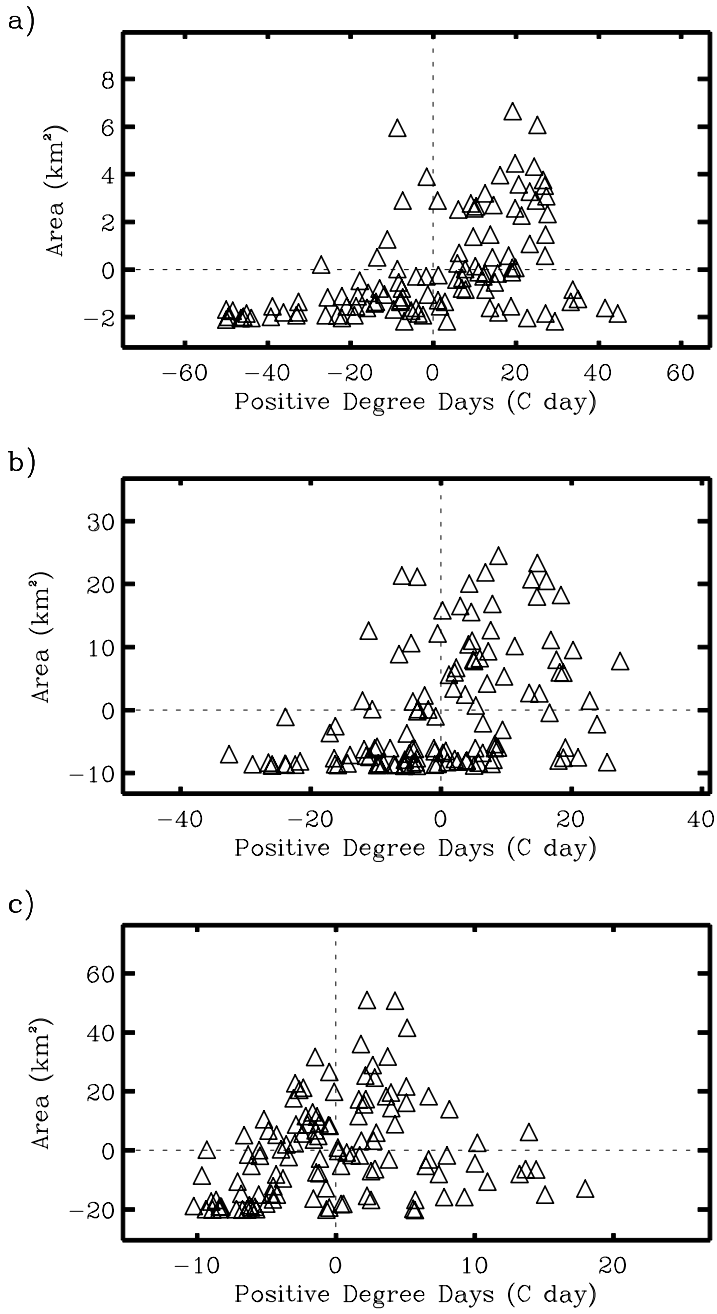

Figure 14. Melt lake area anomalies versus Positive Degree Day (PDD) anomalies for a) Zone 1 (585 - 834 m), b) Zone 2 (835 – 1084 m) and c) Zone 3 (835 – 1334 m).

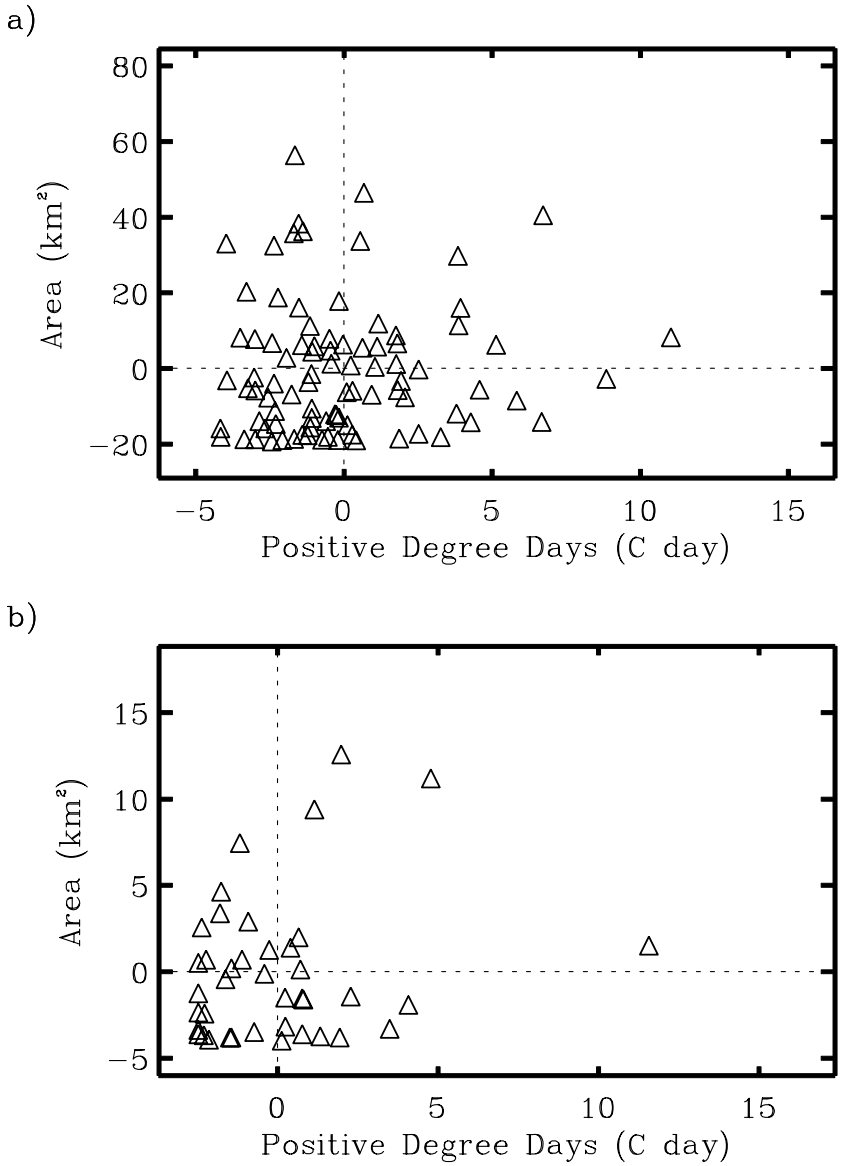

Figure 15. Melt lake area anomalies versus Positive Degree Day (PDD) anomalies for a) Zone 4 (1335 - 1584 m) and b) Zone 5 (1585 – 1834 m).

Melt intensity anomalies are in the ±5°C range, from +0.6°C and -1.8°C for Zone 4 and Zone 5, respectively (Figure 15). Scatter in area and melt intensity anomalies suggests that melt area sensitivity to melt intensity is low at higher elevations, that is,

Zones 4 and 5 (1335 – 1834 m). Area anomalies seem to be less sensitive to melt intensity with increasing elevation. The magnitude of melt area anomalies variability increases with a decrease in PDD anomaly variability. A consistent though slightly smaller correlation between melt intensity and lake volume is evident (not shown).

CHAPTER 6

MELT LAKE TEMPORAL VARIAIBLITY

At 1585 – 1834 m elevation (Zone 4) melt formation occurs roughly 5 weeks later than in the lowest zone (Figure 16). The JAR melt season, on average, begins in early June between 585 – 834 m and in late July between 1585 – 1834 m. A near-linear rise in onset date from 585 – 1584 m elevation is evident. Above 1584 m, in Zone 5, onset date increases by more than 30 days from Zone 4.

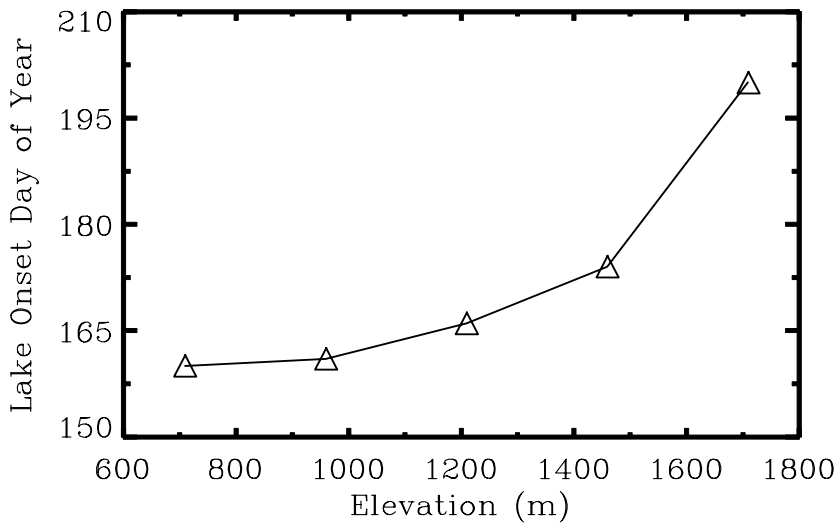

Figure 16. Average date of lake onset versus elevation for Elevation Zones 1 through 5 (585m to 1835m) for 2000 – 2008.

The date of peak area occurs 50 days later in Zone 5 than at Zone 1 (Figure 17). Maximum area occurs more quickly from the onset date in the lowest three zones (~15 days) than at the uppermost zone (~25 days). Corresponding maximum areas for zones 2 and 3 is 33.4 km^2 and 71.2 km^2, respectively.

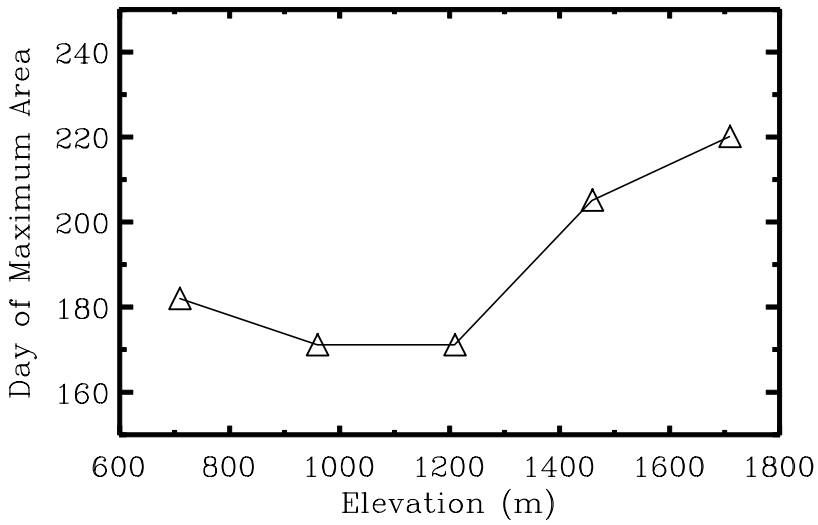

Figure 17. Day of year of lake maximum areal extent versus elevation for elevation zones 1 through 5 (585m to 1835m) for 2000 – 2008.

Figure 18 illustrates lake maximum volume occurring later and later in the melt season with increasing elevation. The date of maximum volume increases from day 160 in Zone 1 to day 220 in Zone 5; a difference of two months.

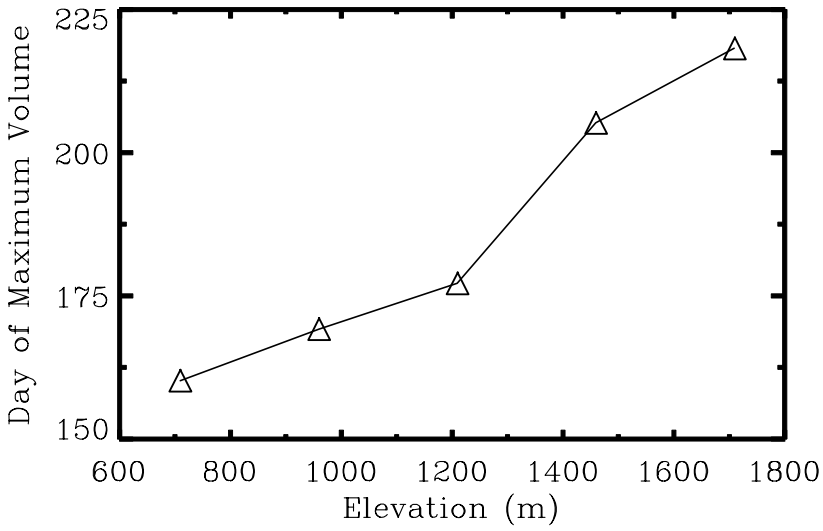

Figure 18. Multi-year (2000 – 2008) average day of year of lake maximum volume versus elevation for Elevation Zones 1 through 5 (585m to 1835m).

The time span for Zone 1 to reach maximum volume after onset (~5 days) is less than the time required for Zone 5 to reach maximum area (~20 days). This suggests that there is larger topographic variability at 585 – 834 m elevation which forces melt water to collect in deeper undulations rather than forming as wide and shallow lakes.

Melt season duration (Figure 19) is the difference between the onset of the melt season and the last day for which melt is observed.

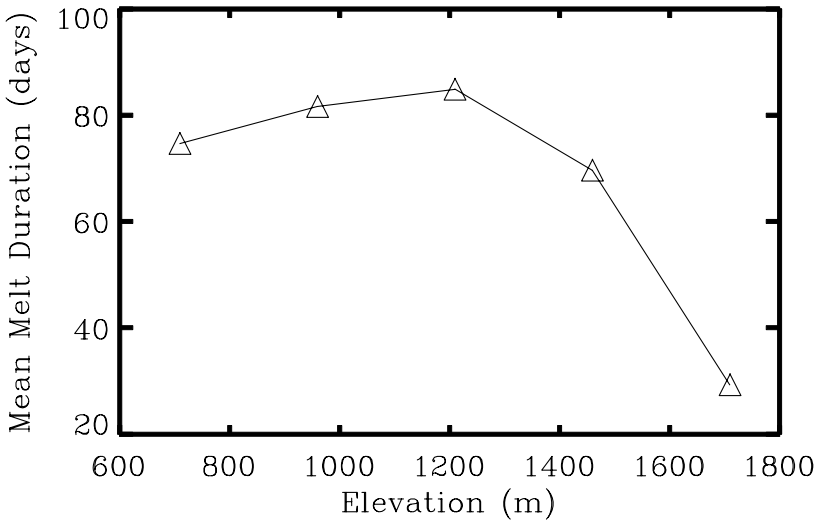

Figure 19. 2000 – 2008 mean melt season duration (days) versus elevation for elevation Zones 1 through 5.

Averaged melt lake duration remains consistent in the lowest four zones, between 70 – 85 days, while the lake season in the uppermost zone lasts an average of 30 days (Figure 19). Because melt lakes develop over time (Box and Ski, 2007), a longer melt season at lower elevations (585 – 1584 m) suggests that there is time for lake formation and drainage to occur and, over time, produce more melt water.

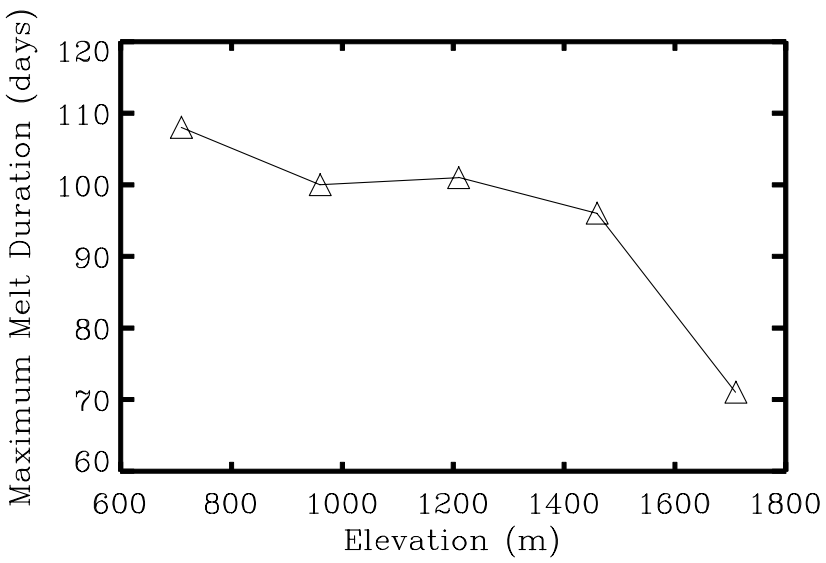

Figure 20. Zonal maximum melt season duration (days) versus elevation for 2000 - 2008.

Maximum duration occurs at 585 – 834 m elevation of 108 days. Maximum duration then decreases with increasing elevation, with a minimum occurring at the uppermost elevation of 71 days. Figure 20 illustrates duration for melt water production for each zone. Warmer melt seasons increase melt season duration between 20 – 24 days.

CHAPTER 7

INDIVIDUAL LAKE DRAINAGE FREQUENCY

For further insight to the spatial and temporal characteristics of melt lakes at JAR, 16 melt lakes are identified and analyzed for 2000 – 2008 (Figure 21). Table 7 illustrates distribution of melt lakes by elevation and latitudinal extent.

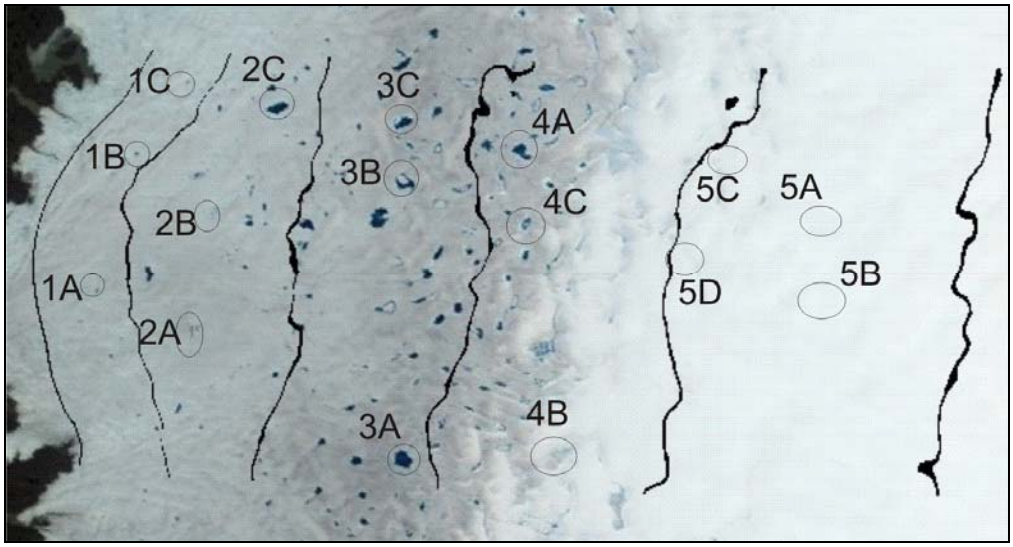

Figure 21. Individual melt lakes (n = 16) at JAR (1A – 5D) as seen by MODIS on day 175 in 2003.

Lake	Elevation (m)	Latitude	Longitude
1A	757	68.4577	-50.1568
1B	799	68.6529	-50.0289
1C	764	68.7447	-49.8671
2A	957	68.4069	-49.7798
2B	934	68.5664	-49.7376
2C	1020	68.7226	-49.4836
3A	1289	68.2353	-48.9684
3B	1231	68.5605	-48.9897
3C	1223	68.7115	-48.9995
4A	1365	68.6768	-48.5474
4B	1462	68.2384	-48.4024
4C	1399	68.5250	-48.5313
5A	1697	68.6208	-47.4215
5B	1728	68.4194	-47.3525
5C	1588	68.6716	-47.8005
5D	1608	68.5234	-47.9058

Table 7. Sixteen melt lakes at JAR, with elevation and coordinates where elevation and coordinates are determined from average maximum depth from 2000 – 2008.

Frequency (N) is the count of lake formation during the 2000 – 2008 period (Figure 22). N decreases with elevation by a rate of 1 year per 200 m of elevation. A higher N occurs for lakes at lower elevations, with lakes in Zone 1 (1A, 1B and 1C) appearing nearly every year while lakes at higher elevation (1585 – 1834 m) forming, on average, twice, from 2000 – 2008. Lakes with lower frequency (N < 4) form in later years (2003 – 2008).

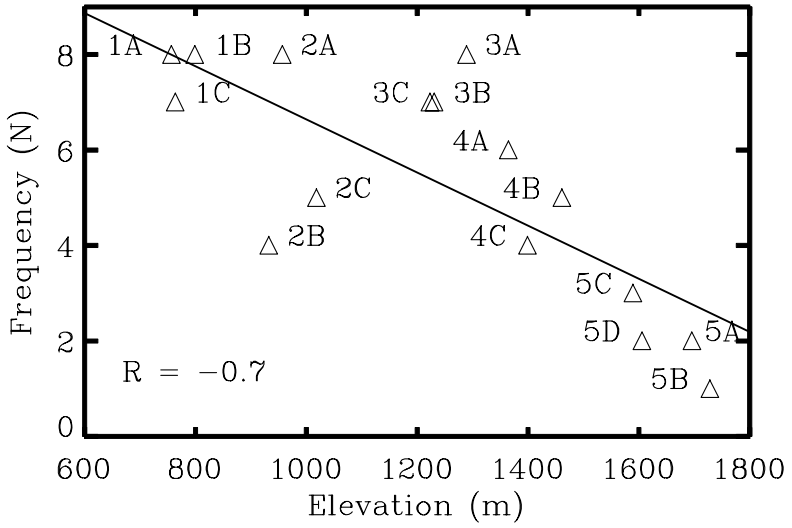

Figure 22. Frequency (N) of lakes that appear in JAR between 2000 – 2008.

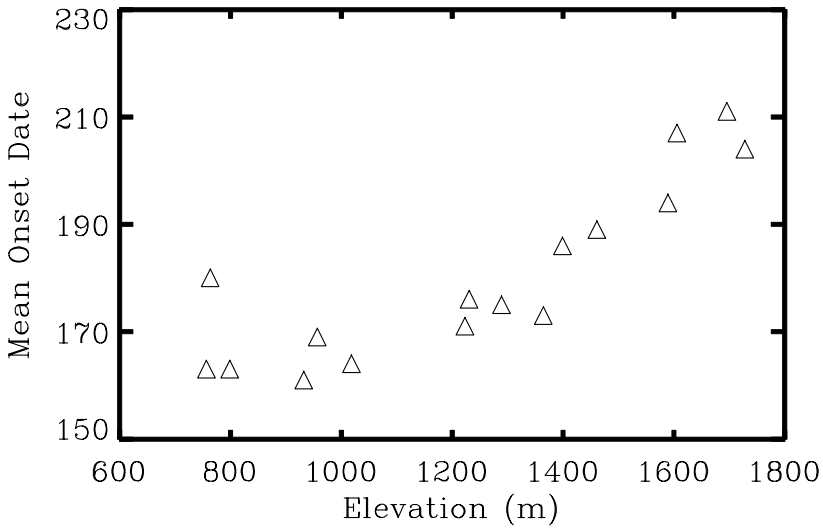

Figure 23. Mean onset date for Lakes 1A – 5D versus elevation.

Mean individual lake onset date occurring earlier at lower elevations confirms the zonal melt season begins later at higher elevations (Figure 23). At the highest elevation (1728 m) the melt season begins on day 223, while on day 193 at the lowest elevation (757 m); a difference of 30 days. Melt lake onset occurs later at higher elevation lakes at a rate of ~4.2 days per 100 m between 757 – 1728 m.

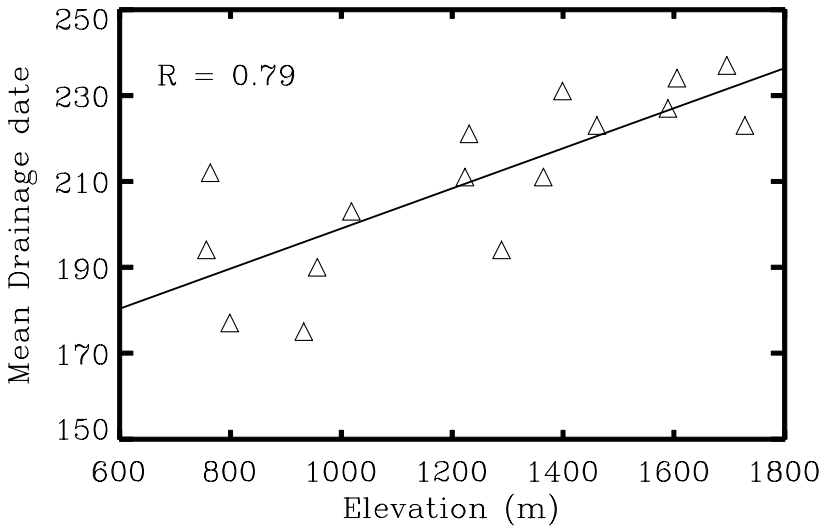

Figure 24. Mean drainage date for Lakes 1A – 5D versus elevation.

Individual lakes at lower elevation begin earlier (~180) than at higher elevation (~245) (Figure 24). The slope of the drainage date-versus-elevation line suggests that drainage date increases at a rate of 4.6 days per 100 m between 757 – 1728 m. Temporal variability of individual lake drainage is greatest at the lowest zone (Lakes 1A, 1B and 1C). Variability decreases with elevation, with the closest range in drainage date at the uppermost lakes (Lakes 5A, 5B, 5C and 5D).

Draining date variability is dependent on the length of the melt season. Longer melt seasons (Figure 19) induce greater variation in drainage dates, while shorter melt seasons induce smaller variability in individual lake drainage.

The McMillan et al. (2007) conclusion that all runoff is caught in melt lakes and no drainage occurring before day 188 is misleading. In this study 24 drainage events, between 755 – 1367 m elevation, occurred before day 188 (2000 – 2008). The highest

concentration of these drainage events took place in 2003 and 2007, each with 7 drainage events in that year. No individual drainage events, however, are found before day 188 in 2001, supporting the initial conclusion of McMillan et al. (2007). Individual drainage results suggest that some lakes can drain immediately after the onset of the melt season.

CHAPTER 8

WARMING CLIMATE IMPLICATIONS

Supra-glacial melt lakes provide a water reservoir and a delay factor in water delivery to the internal hydraulic system. Maximum melt water volume at JAR during the 2000 – 2008 period is 0.45 km^3. Duration of the melt season not only changes with elevation (30 – 80 days), but has the capacity to double in length in warmer melt seasons (70 – 110 days). Longer melt seasons would increase in melt area and volume quantities. Individual lakes not only reappear each year, but their zonal surface coverage is greater in relatively warm time-periods. Melt lakes also have the potential to drain early in the melt season (< day 188). Thus, the Lüthje et al. (2006) conclusion that there are insufficient MODIS data to determine melt lake trends is misleading.

A projected climate warming scenario of 3 – 5°C by 2100 (IPCC, 2007) would increase zonal melt intensity and enhance melt water availability. The increase in melt water production would lead to an increase in larger, more numerous supra-glacial melt lakes at JAR. In this warming scenario, it is anticipated that the maximum melt water production at 1085 – 1584 m elevation will expand to include elevations of 1835 m

(Zone 5) or higher. A climate warming scenario suggests that conditions currently at JAR will expand toward higher elevations and latitudes.

In a warming climate, the ELA is expected to shift towards the interior of the ice sheet. The migration of the ELA would heighten surface undulation formation by raising the elevation at which the surface becomes predominately bare ice. The change in surface type is expected to increase melt lake development and enhance the mass loss component in Greenland's hydrologic budget and further accelerate sea level rise.

REFERENCES

Abdalati, W. and K. Steffen. 2001. Greenland ice sheet melt extent: 1979-1999. *J. Geophys. Res.*, **106**, 33983-33988

Alley, R.B.,T.K. Dupont, B.R. Parizek and S. Anandakrishnan. 2005. Access of surface melt water to bed of subfreezing glaciers: preliminary insights. *Ann Glaciol.*, **40**, 8-14.

Boon, S. and M. Sharp. 2003. The role of hydrologically-driven ice fracture in drainage system evolution on an Arctic glacier. *Geophys. Res. Lett.,* **30**(18), 1916.

Box, J.E., J.F. Heinrichs, and J. Key. 1997. An arctic surface radiation budget climatology from in-situ and satellite derived data. *International Radiation Symposium*. Fairbanks, AK

Box, J.E. and K. Steffen. 2001. Sublimation estimates for the Greenland ice sheet using automated weather station observations, *J. of Geophys. Res.*, 106(D24), 33965-33982

Box, J.E. 2002. Survey of Greenland instrumental temperature records: 1873–2001. *Int. J. Climatol.* **22**: 1829–1847

Box, J.E., D. H. Bromwich and L-S Bai. 2004. Greenland ice sheet surface mass balance for 1991-2000: application of Polar MM5 mesoscale model and in-situ data. *J. Geophys. Res.*, **109**, D16105.

Box, J.E., D.H. Bromwich, B.A. Veenhuis, L-S Bai, J.C. Stroeve, J.C. Rogers, K. Steffen, T. Haran, S-H Wang, 2006. Greenland ice sheet surface mass balance variability (1988-2004) from calibrated Polar MM5 output, *Journal of Climate,* Vol. 19, No. 12, pp. 2783–2800.

Box, J. E. and K. Ski. 2007. Remote sounding of Greenland supra-glacial melt lakes: implications to sub-glacial hydraulics. *J. Glaciol.,* **181**, 257 – 265.

Braithwaite, R.J. and O.B. Oleson. 1989. Calculation of glacier ablation from air temperature, West Greenland. In Oerlemans, J., ed. Glacier Fluctuations and dimatic Change. Dordrecht etc. Kluwer Academic Publishers, 219 – 233.

Braithwaite, R.J. 1995. Positive degree-day factorsfor ablation on the Greenland ice sheet studied by energy balance modelling. *J. Glaciol.*, 41(137), 153 – 160.

Bromwich, D.H., J.J. Cassano, T. Klein, G. Heinemann, K.M. Hines, K. Steffen and J.E. Box. 2001. Mesoscale modeling of katabatic winds over Greenland with the Polar MM5, *Mon. Weather Rev.*, **129,** 2290-2309.

Bryzgis, G. and J.E. Box 2005. West Greenland ice sheet melt lake observations and modeling. *EOS Trans. AGU*, **86**, C41A07.

Cassano, J.J., J.E. Box, D.H. Bromwich, L. Li and K. Steffen. 2001. Evaluation of Polar MM5 simulations of Greenland's atmospheric circulation, *J. Geophys. Res.* 106, D24, 33867 – 33889.

Chen J.L., C.R. Wilson, and B.D. Tapley. 2006. Satellite gravity measurements confirm accelerated melting of Greenland ice sheet. *Science*. 313, 1958-60.

Church, J. A., J.M. Gregory, P. Huybrechts, M. Kuhn, K. Lambeck, M.T. Nhuan, D. Qin, P.L. Woodworth, O.A. Anisimov, F.O. Bryan, *et al.* (2001) in *Climate Change 2001: The Scientific Basis (Contribution of Working Group I to the Third Assessment Report of the Intergovernmental Panel on Climate Change)*, eds. Houghton, J. T., Y. Ding, D.J. Griggs, M. Noguer, P.J. van der Linden, X. Dai, K. Maskell, and C.A. Johnson, (Cambridge Univ. Press, Cambridge, U.K.), pp. 639-694.

Curry, J.A., J.L. Schramm and E.E. Ebert. 1995. Sea ice–albedo climate feedback mechanism. *J. Climate,* **8**(2), 240–247.

Das S. B., I. Joughin, M.D. Behn, I.M. Howat, M.A. King, D. Lizarralde, M.P. Bhatia. 2008. Fracture propagation to the base of the Greenland ice sheet during supraglacial lake drainage, *Science*, 320, 778-781.

Echelmeyer, K. and W.D. Harrison. 1990. Jakobshavn Isbræ, West Greenland—Seasonal variations in velocity or lack thereof. *J. Glaciol*. 36, 82–88.

Ekholm, S. 1996. A full coverage, high-resolution, topographic model of Greenland computed from a variety of digital elevation data. *J. Geophys. Res. – solid Earth*. 101, (B10), 21961-21972.

Fichefet, T., C. Poncin, H. Goosse, P. Huybrechts, I. Janssens, and H. Le Treut. 2003. Implications of changes in freshwater flux from the Greenland ice sheet for the climate of the 21st century, *Geophys. Res. Lett.*, **30**(17), 1911.

Fettweis, X. 2007. Reconstruction of the 1979–2006 Greenland ice sheet surface mass balance using the regional climate model MAR. *The Cryosphere Discussions*, 1, 123-168.

Gerdel, R.W. and F. Drouet. 1960. The Cryoconite of the Thule Area, Greenland, Transactions of the American Microscopical Society, **79**(3). Jul., 1960, pp. 256-272.

Gumley, L., J. Descloitres and J. Schmaltz. 2003. Creating reprojected true color MODIS images: A tutorial: http://rapidfire.sci.gsfc.nasa.gov/faq/MODIS_True_Color.pdf

Hall, D.K., R.S. Williams, S.B. Luthke, N.E. Degirolamo. 2008. Greenland ice sheet surface temperature, melt and mass loss: 2000-2006. *J. Glaciol.* **54**(184), 81-93.

Holland, D. M., R. H. Thomas, B. de Young, M. H. Ribergaard, and B. Lyberth, 2008. Acceleration of Jakobshavn Isbrae triggered by warm subsurface ocean waters. *Nature Geosci.*, 1, doi:10.1038/ngeo316

Howat, I. M., I. Joughin and T. Scambos. 2007. Rapid changes in ice discharge from Greenland outlet glaciers, *Science,* 315, 1559.

IPCC, 2007: Summary for policymakers. In: *Climate Change 2007: The Physical Science Basis. Contribution of Working Group I to the Fourth Assessment Report of the Intergovernmental Panel on Climate Change* [Solomon, S., D. Qin, M. Manning, Z. Chen, M. Marquis, K.B. Averyt, M.Tignor and H.L. Miller (eds.)]. Cambridge University Press, Cambridge, United Kingdom and New York, NY, USA.

Joughin, I., S. Tulaczyk, M. Fahnestock and R. Kwok. 1996. A mini-surge on the Ryder Glacier, Greenland, observed by satellite radar interferometry. *Science*, **274**, 228–230.

Joughin, I., S. Das, M. King, B. Smith, I. Howat and T. Moon. 2008a. Seasonal speedup along the western flank of the Greenland ice sheet, *Science*, **320**, 781 – 783. doi: 10.1126/science.1153288

Joughin, I., I. M. Howat, M. Fahnestock, B. Smith, W. Krabill, R. Alley, H. Stern, and M. Truffer. 2008b. Continued evolution of Jakobshavn Isbrae following its rapid speedup, *Journal of Geophysical Research*, 113, F04006, doi:10.1029/2008JF001023

Krabill, W., E. Hanna, P. Huybrechts, W. Abdalati, J. Cappelen, B. Csatho, E. Frederick, S. Manizade, C. Martin, J. Sonntag, R. Swift, R. Thomas and J. Yungel,

2004. Greenland ice sheet: Increased coastal thinning, *Geophys. Res. Lett.*, 31, L24402

Lüthje M., L.T. Pedersen, N. Reeh, and W. Greuell, 2006. Modelling the evolution of supra-glacial lakes on the West Greenland ice-sheet margin. *Journal of Glaciology.*, **52**, 608-618.

McMillan M., P. Nienow, A. Shepherd, T. Benham, and A. Sole, 2007. Seasonal evolution of supra-glacial lakes on the Greenland ice sheet. *Earth and Planetary Science Letters*, **262**, 484-492.

Ohmura, A. and N. Reeh. 1991. New precipitation and accumulation maps for Greenland. *J. Glacial.* 37, 140-148.

Ohmura, A., P. Calanca, M. Wild, and M. Anklin. 1999. Precipitation, accumulation and mass balance of the Greenland Ice Sheet, *Zeitshrift fuer Gletscherkunde und Glaciologie, Universitaetsverlag Wagner, Innsbruck, Band 35, Heft 1*, 1-20.

Parizek, B. and R.B. Alley. 2004. Implications of increased Greenland surface melt under global-warming scenarios: ice-sheet simulations. *Quaternary Science Reviews*, 23, 1013-1027

Paterson, W.S.B. 1994. The physics of glaciers. 3rd Edition. Oxford, New York, Tokyo, Pergamon, ix, 480 pp. ISBN 0-08037945 1, HB. ISBN 0-08037944 3, Flexicover.

Perovich, D.K., W.B. Tucker, III and K.A. Ligett. 2002. Aerial observations of the evolution of ice surface conditions during summer. *J. Geophys. Res.,* 107(C10), 8048.

Reeh, N., C. Mayer, H. Miller, H.H. Thomsen, and W. Weidick. 1999. Climate control on fjord glaciations in Greenland: implications for IRD-deposition in the sea. *Geophys. Res. Lett.* **26** 8, pp. 1039–1042.

Rignot, E. and P. Kanagaratnam. 2006. Changes in the velocity structure of the Greenland ice sheet. *Science*. **311**, 986-990.

Rignot, E., J.E. Box, E. Burgess, and E. Hanna. 2008. Mass balance of the Greenland ice sheet from 1958 to 2007, *Geophys. Res. Lett.*, 35, L20502.

Scambos, T. A., C. Hulbe, M. Fahnestock, and J. Bohlander. 2000. The link between climate warming and break-up of ice shelves in the Antarctic Peninsula, *J. Glaciol.*, 46, 516–530.

Shepherd, A., A. Hubbard, P. Nienow, M. King, M. McMillan, and I. Joughin. 2009. Greenland ice sheet motion coupled with daily melting in late summer, *Geophys. Res. Lett.*, 36, L01501.

Sneed,W.A. and G.S. Hamilton. 2007. Evolution of melt pond volume on the surface of the Greenland Ice Sheet. *Geophysical Research Lett*ers **34**, L03501.

Solomonson V., W. Barnes, P. Maymon, H. Montgomery and H. Ostrow. 1989. MODIS: Advanced Facility Instrument for Studies of the Earth as a System, *IEEE Trans. Geosci. and Remote Sensing,* 27,145-153.

Steffen, K. and J.E. Box. 2001. Surface climatology of the Greenland ice sheet: Greenland Climate Network 1995-1999. *J. of Geophys. Res.***106**(24), 33951-64.

Thomas, R., W. Abdalati, E. Frederick, W. B. Krabill, S. Manizade, and K. Steffen, 2003. Investigation of surface melting and dynamic thinning on Jakobshavn Isbræ, Greenland, J. Glaciol., 49, 231-239.

van der Veen, C. J. 1998. Fracture mechanics approach to penetration of surface crevasses on glaciers, *Cold Regions Sci. Technol.*, 27, 31–47.

van den Broeke, M. R., C. J. P. P. Smeets and J. Ettema, C. van der Veen, R. S. W. van de Wal and J. Oerlemans, 2008: Partitioning of energy and meltwater fluxes in the ablation zone of the west Greenland ice sheet, *The Cryosphere* 2, 179-189.

Vieli, A., J. Jania, H. Blatter and M. Funk. 2004. Short-term velocity variations on Hansbreen, a tidewater glacier in Spitsbergen. *J. Glaciol.*, **50**(170), 389–398.

Weidick, A., N. Mikkelsen, C. Mayer and S. Podlech. 2004. Jakobshavn Isbræ, West Greenland: the 2002-2003 collapse and nomination for the UNESCO World Heritage List, in: Sønderholm, M. & Higgins, A.K.(eds): Review of Survey activities 2003, Geological Survey of Denmark and Greenland Bulletin, 4, 85-88.

Weidick, A. and O. Bennike,: Quaternary glaciation history and glaciology of Jakobshavn Isbræ and the Disko Bugt region, West Greenland: a review, Geological Survey of Denmark and Greenland, Bulletin 14, 80 pp, 2007.

Zwally, J. H. and M.B. Giovinetto. 2001. Balance mass flux and ice velocity across the equilibrium line in drainage systems of Greenland. *J. Geophys. Res.*, **106**(33) 717–33.

Zwally, H.J., W. Abdalati, T. Herring, K. Larson, J. Saba and K. Steffen. 2002. Surface melt-induced acceleration of Greenland ice-sheet flow. *Science*, **297**, 218-222.